ACS Catalysis

pubs.acs.org/acscatalysis

Research Article

Ru-Catalyzed Isomerization of Achmatowicz Derivatives: A Sustainable Route to Biorenewables and Bioactive Lactones

Miroslav Dangalov,[⊥] Adolfo Fernández-Figueiras,[⊥] Martin A. Ravutsov, Ekaterina Vakarelska, Maya K. Marinova, Nuno R. Candeias, and Svilen P. Simeonov*

Cite This: *ACS Catal.* 2023, 13, 1916–1925

Read Online

ACCESS | Metrics & More | Article Recommendations | Supporting Information

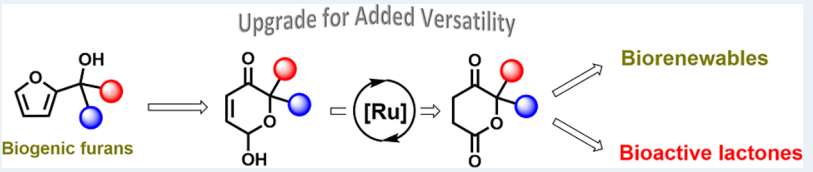

ABSTRACT: A Ru-catalyzed isomerization of Achmatowicz derivatives that opens unexplored routes to diversify the biogenic furanic platform is reported. The mechanistic insights of this formally redox-neutral intramolecular process were studied computationally and by deuterium labeling. The transformation proved to be a robust synthetic tool to achieve the synthesis of bioderived-monomers and a series of 4-keto-δ-valerolactones that further enabled the development of a flexible strategy for the synthesis of acetogenins. A concise and protective group-free asymmetric total synthesis of two natural products, namely, (*S*,*S*)-muricatacin and the (*S*,*S*)-L-factor, is also described.

KEYWORDS: *ruthenium catalysis, allylic alcohol isomerization, Achmatowicz rearrangement, biorefinery, bioactive lactones*

INTRODUCTION

The biogenic furanic platform is considered to be a promising sustainable source of chemicals,[1−3] for example, for the manufacture of resins and biofuels.[3,4] Among other transformations that exploit this platform, the Achmatowicz rearrangement proved to be an efficient synthetic tool to produce structurally complex derivatives from simple furans and thus holds a unique place in the synthesis of many natural products and diverse organic syntheses.[5−11] Its potential to serve as a key step in the production of biomass-derived C5 alcohols was recently reported by our group.[12,13]

The exploitation of the densely functionalized Achmatowicz dihydropyranones in organic synthesis has been reported in many instances.[14,15] The hemiacetal and ketone groups received particular attention as numerous oxidations of the hemiacetal[16−18] and reductions of the ketone group[17−19] have been reported. To a lesser extent, the reduction of the olefin has also been described.[12,20,21]

The redox isomerization of allylic alcohols into saturated carbonyl compounds is among the most well-studied transition-metal-catalyzed processes.[22,23] The development of efficient catalysts[24−27] for this transformation showcased impressive advances; however, the majority of the reported examples have been devoted to the synthesis of simple α- and/or β-branched aldehydes and ketones. Despite their obvious utility,[28] synthetic strategies that harness transition metal-catalyzed redox isomerization in the context of Achmatowicz derivatives have been scarcely described. Aiming at an expedient synthesis of carbohydrates, Wang et al. reported an Ir-catalyzed dynamic kinetic redox isomerization of Achmatowicz derivatives.[29] This approach involves oxidation of the hemiacetal and consequent diastereoselective reduction of the ketone (Scheme 1A) and provided access to the key intermediates (**1**) in the synthesis of naturally occurring sugars. Later on, the same isomerization has been achieved by employing an enantioconvergent biocatalytic approach to yield γ-hydroxy-δ-lactones in an enantio- and diastereoselective fashion (Scheme 1B). The transformation has been shown to proceed also in vivo.[30,31]

To the best of our knowledge, transformations that utilize the reduction of the olefin instead of the ketone in a redox isomerization of Achmatowicz dihydropyranones still have not emerged. Herein, we present a new highly efficient Ru-catalyzed isomerization of a range of Achmatowicz derivatives to 4-keto-δ-valerolactones (**2**) by consecutive oxidation of the hemiacetal and reduction of the olefin. This strategy enabled the preparation of biorenewable monomers and a series of bioactive lactones (Scheme 1C).

Received: October 4, 2022
Revised: January 3, 2023
Published: January 18, 2023

Scheme 1. Redox Isomerization of Achmatowicz Derivatives and Downstream Applications

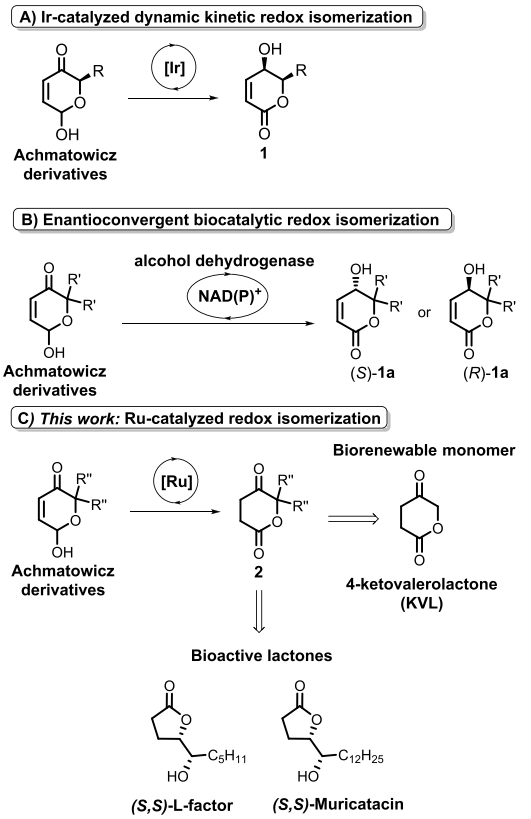

RESULTS AND DISCUSSION

We began our studies using 10 mol % [Ir(*cod*)MeO]$_2$ as a catalyst. In the absence of a ligand, we observed full conversion of the starting material **3.** The desired product **4** was formed in low yields alongside the formation of two major side products (Scheme 2), namely, **5**, arising from the reduction of the ketone, and the oxidized product **6** (Table 1, entry 1). We were not able to identify other reaction products, and thus we anticipated that this was due to the occurrence of undesired polymerization reactions in which products could not be elucidated by NMR spectroscopy or detected by GC analysis.

Scheme 2. Redox Isomerization of 6-Hydroxy-2*H*-pyran-3(6*H*)-one 3

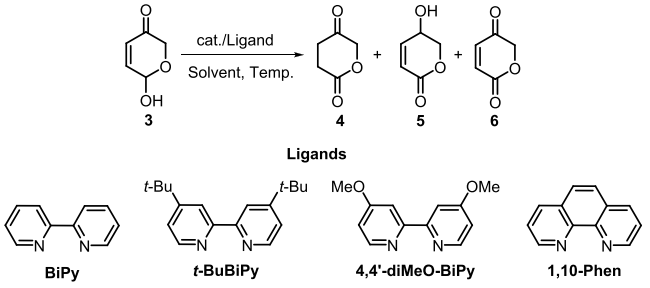

The use of *t*-Bu-BiPy and BiPy as ligands rendered product **4** in high yields of 84 and 85%, respectively (Table 1, entries 2 and 3). Noteworthy, the formation of the side products **5** and **6** was not detected. However, we still experienced a 16% unidentified loss of yield. The use of 4,4′-diMeO-BiPy or 1,10-phenanthroline ligands did not provide a positive effect (Table 1, entries 4 and 5). Unfortunately, our further attempts to solve that issue using [Ir(*cod*)MeO]$_2$ as a catalyst failed under various reaction conditions (see Supporting Information 1, Table S1, entries 1−19).

Despite the fact that, in several instances, the [Ir(*cod*)-MeO]$_2$/BiPy catalyst provided **4** in very high yields (Table S1, entries 6, 7, and 12−14), the high catalyst loading and the unidentifiable loss of yield provoked us to continue our studies by screening a series of other catalysts. In this series, [Ir(*cod*)Cl]$_2$, Pd(OAc)$_2$, Pd$_2$(dba)$_3$, and [Ru(*cod*)Cl$_2$]$_n$ were found to be ineffective under various conditions (Table S1, entries 20−26). Although, in some instances, the formation of **4** was observed in the presence of Ru(CO)(H)(Ph$_3$P)$_3$Cl or [Ru(p-cymene)Cl$_2$]$_2$, the yields have been far from satisfactory (Table S1, entries 27−37). The use of 2 mol % [RuCp*-(MeCN)$_3$]PF$_6$ in THF rendered a more promising 70% yield of **4** (Table 1, entry 6). To our delight, **4** was formed in nearly quantitative analytical yields when the reaction was performed in refluxing MeCN (Table 1, entry 7). Noteworthy, this was the first experiment in which significant degradation of the starting material and/or the reaction products was not observed. The yield was reproducible in the presence of only 1 mol % catalyst (Table 1, entry 8). However, the decrease of the catalyst loading to 0.5 mol % rendered **4** in an 89% yield (Table 1, entry 9).

The 4-keto-*δ*-valerolactone (KVL) **4** has been previously reported from levulinic acid (LA) as a biorenewable monomer for the production of chemically recyclable and biodegradable polymer poly(4-ketovalerolactone) (PKVL).[32] Such an approach utilizes 5-bromo levulinic acid (5-BrLA) as an intermediate, thus requiring extensive use of Br$_2$. Furthermore, due to the availability of several activated positions, the regioselective bromination of LA proved to be troublesome and rendered a mixture of regioisomers and bis-brominated products.[32]

Stepping on the availability of **3** and our previous work on its upscale synthesis under flow conditions,[12] we achieved the gram scale production of **4** in up to 87% of isolated yield (Table 1, entries 10 and 11). In contrast to the previous methods that rendered up to a 40% yield from LA, the overall yield of **4** from furfuryl alcohol was >80%. Noteworthy, our strategy is much more atom-efficient due to the lack of regioselectivity issues and extensive use of halogens.

To investigate the scope of the Ru-catalyzed isomerization (Scheme 3), we prepared a variety of alkyl-substituted Achmatowicz derivatives, namely, **7a−7l**. In this series, we observed that the reaction rate was governed by the length of the substituent. The methyl- and ethyl-substituted lactones **8a** and **8b** were obtained in excellent yields in the 3 h reaction time. The *n*-pentyl **8c** and phenethyl **8d** derivatives were converted in only 30 and 35% isolated yields after 24 h, respectively, whereas the remaining starting material was predominantly preserved. The steric bulk of *i*-Pr **7e** and cyclohexyl **7f** derivatives was reflected in prolonged reaction times; however, the corresponding lactones **8e** and **8f** were obtained in excellent yields. The reaction tolerates a variety of other substituents including allyl (**8g**), spiro (**8h−8j**), and disubstituted derivatives (**8k** and **8l**).

We attempted to gain deeper understanding of the unusual effect of the length of the substituents by means of 2D ^{1}H−^{1}H NOESY NMR experiments. Unfortunately, the NMR data did not provide conclusive information on the proximity of those substituents to the reactive protons from the allylic system.

https://doi.org/10.1021/acscatal.2c04867
ACS Catal. 2023, 13, 1916−1925

Table 1. Catalytic Experiments[a,b]

entry	catalyst	loading (mol %)	solvent	temp (°C)	ligand (mol %)	time (h)	**3** (%)	**4** (%)	**5** (%)	**6** (%)
1	[Ir(*cod*)MeO]$_2$	10	DCE	60		1		18	3	26
2	[Ir(*cod*)MeO]$_2$	10	DCE	rt	*t*-Bu-BiPy (10)	1		84		
3	[Ir(*cod*)MeO]$_2$	10	DCE	60	BiPy (10)	1		85		
4	[Ir(*cod*)MeO]$_2$	10	DCE	60	4,4′-diMeO-BiPy (10)	1	6	61		
5	[Ir(*cod*)MeO]$_2$	10	DCE	60	1,10-Phen (10)	1	53	27		
6	[RuCp*(MeCN)$_3$]PF$_6$	2	THF	reflux		4		70		
7	[RuCp*(MeCN)$_3$]PF$_6$	2	CH_3CN	reflux		4		99		
8	[RuCp*(MeCN)$_3$]PF$_6$	1	CH_3CN	reflux		6		99		
9	[RuCp*(MeCN)$_3$]PF$_6$	0.5	CH_3CN	reflux		6		89		
10	[RuCp*(MeCN)$_3$]PF$_6$	1	CH_3CN	reflux		17		87[c,d]		
11	[RuCp*(MeCN)$_3$]PF$_6$	1	CH_3CN	reflux		18		85[c,e]		

[a]Yields determined by GC analysis using dodecane as an internal standard. [b]0.5 mmol **1** in 5 mL of solvent. [c]Yield after chromatographic purification. [d]gram scale (**3** = 1.14 g, 10 mmol). [e]gram scale (**3** = 2.28 g, 20 mmol).

Scheme 3. Scope of the Ru-Catalyzed Isomerization[a,b]

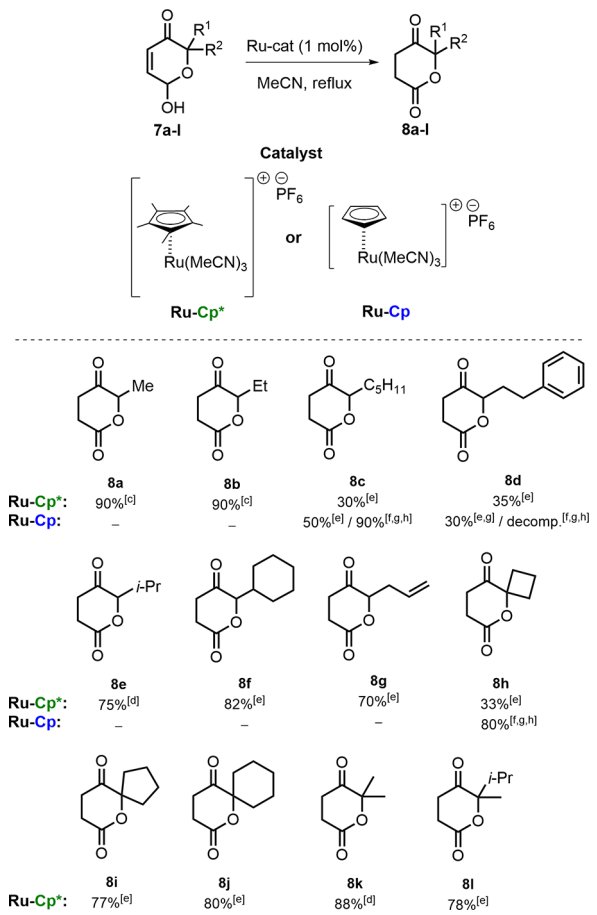

[a]Reactions were monitored by TLC. [b]Yields after chromatographic purification; [c]3 h; [d]18 h; [e]24 h; [f]48 h; [g]2 mol % cat.; [h]130 °C, Synthware pressure vessel.

However, the experimental data supported the involvement of steric effects.

The exposure of **7c** to the less sterically bulky complex [RuCp(MeCN)$_3$]PF$_6$ rendered the corresponding lactone **8c** in an improved 50% yield (Scheme 3), indicating that the steric bulk of the catalyst plays an important role; however, this role was not dominant. This finding led us to elevate the catalyst loading and the reaction temperature (2 mol %, 130 °C). To our delight, this resulted in a significant improvement, leading to the formation of **8c** in an excellent yield of 90%. Due to decomposition at high temperatures, our attempt to increase the yield of the phenethyl derivative **8d** was unsuccessful. On the other hand, the increased catalyst loading alone did not provide a pronounced effect. Furthermore, spiro lactone **8h**, which was previously obtained in only 33%, was isolated in an 80% yield. Finally, we performed a gram-scale isomerization of Achmatowicz derivative **3** under the same conditions used for the [RuCp*(MeCN)$_3$]PF$_6$ catalyst (see Supporting Information 1, Section S2.3.1). Nevertheless, we did not observe any effect of the steric bulk of the catalyst over the reaction rate.

In all the cases, we observed slight decomposition of the products during purification on silica gel (for analytical yields, see Supporting Information 1, Section S2.3.2). Despite the hydrolysis of the lactones being the most obvious cause for the reduced yields, we were not able to identify the formation of the corresponding acids.

Next, we turned our attention to the synthesis of 5-hydroxyalkylbutan-4-olides, which are lactones widespread in nature that exhibit diverse biological properties, such as insect antifeedant activity[33] and anti-tumor activity.[34,35] Members of this family are found in microbial metabolite cultures of *Erwinia quernica*[36] and *Streptomyces griseus*.[37] The short-chain homologues are flavor constituents in alcoholic beverages.[38,39] Given this, it comes as no surprise that much attention has been given to their synthesis and exploitation as synthons in the preparation of complex natural products.[40−44]

We rationalized that a reduction of the ketone in derivatives **8a**−**8k** will deliver simultaneous isomerization of the formed 4-hydroxy-*δ*-valerolactones to the more stable 5-hydroxyalkylbutan-4-olides, thus providing a concise flexible synthetic route to achieve the synthesis of these biologically significant lactones. To our delight upon simple treatment with $NaBH_4$ in DCM in the presence of a catalytic amount of AcOH (Method A), **4** was directly converted in a nearly quantitative yield to lactone **10** without isolation of the intermediate hydroxylactone **9** (Scheme 4).

In the presence of $NaBH_4$, mono-substituted substrates **8a**−**8c** were converted to the corresponding butyrolactones **12a**−**12c** in good to high yields (Scheme 4). In the case of *n*-pentyl lactone **8c**, the increased steric bulk of the substituent hampered the valerolactone to butyrolactone isomerization and we obtained an inseparable mixture of the intermediate hydroxyl lactone **11c** and the desired product in a 65% yield. However, a simple treatment of this mixture with a catalytic amount of aq. HCl in MeOH rendered quantitative isomer-

https://doi.org/10.1021/acscatal.2c04867
ACS Catal. 2023, 13, 1916−1925

Scheme 4. Synthesis of 5-hydroxyalkylbutan-4-olides[a,b]

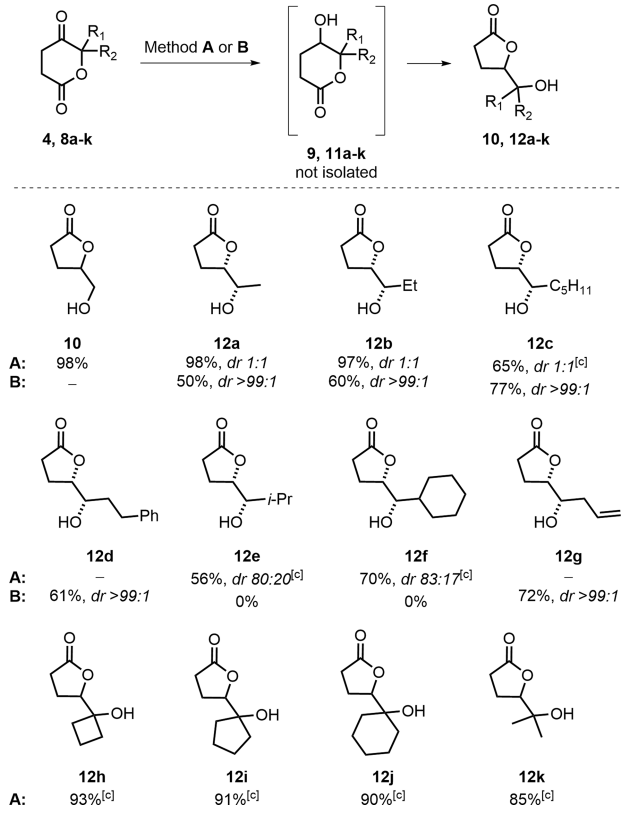

[a]Method A: 2.0 equiv $NaBH_4$, 2 drops of AcOH, DCM, rt, 24 h; [b]Method B: L-selectride, THF, −78 °C; [c]cat. HCl, MeOH, rt, 24 h.

ization to **12c**, which was isolated without further purification. Noteworthy, in all cases, we obtained an inseparable mixture of diastereoisomers in a near 1:1 ratio. The treatment of **8a−8c** with bulkier L-selectride (Method B) delivered products **12a−12c** as single *syn*-diastereoisomers in good yields. The L-selectride reduction reaction does not tolerate bulkier *i*-Pr and cyclohexyl substituents, and we observed the formation of complex mixtures of products. This observation is in accordance with steric effects governing the better diastereoselectivity achieved with L-selectride. However, upon treatment with $NaBH_4$, the desired butyrolactones **12e** and **12f** were achieved in good yields and moderate diastereoselectivity (*dr* = 80:20 and 83:17, respectively). To our delight, the phenethyl **8d** and allyl **8g** substituted derivatives reacted smoothly in the presence of L-selectride. The corresponding lactones **12d** and **12g** were isolated as single *syn*-diastereoisomers in good yields. Noteworthy, one can foresee the latter as a precursor to higher acetogenin synthesis due to the presence of the terminal olefin prone to downstream modifications. Despite the fact that treatment with aq. HCl/MeOH was required, the spiro **8h−8j** and disubstituted derivative **8k** were converted in excellent yields to the corresponding products **12h−12k** in the presence of $NaBH_4$.

Finally, we wanted to demonstrate the utility of our synthetic strategy by its application to the protective-group-free total asymmetric synthesis of two important members of the acetogenin family, namely, L-factor and muricatacin. The L-factor is isolated from *Streptomyces griseus* and is considered an autoregulator of anthracycline biosynthesis.[45] Muricatacin is isolated from the seeds of *Annona muricata* and has received attention in research due to its anti-proliferative activity and cytotoxicity against various human tumoral cell lines.[46,47] It has been intensively exploited as a gateway synthon to higher acetogenin synthesis.[48] To date, the synthetic approaches to achieve the synthesis of these chiral 5-hydroxyalkylbutan-4-olides mainly exploit nature's chiral pool,[49] namely, carbohydrates, which, in many instances, require laborious multistep synthesis and extensive use of protective groups.[50−52] Catalytic asymmetric approaches have been rarely reported and are limited to the use of asymmetric dihydroxylation or epoxidation of synthetic unsaturated carboxylic acids.[49,53,54]

We initiated our asymmetric synthesis from furfuryl alcohols ***S*-14c** and ***S*-14m** that are readily available in their both enantiomeric forms from Noyori asymmetric hydrogenation of the corresponding ketones **13c** and **13m** (Scheme 5).[55,56]

Scheme 5. Asymmetric Synthesis of (+)-L-factor and (+)-Muricatacin

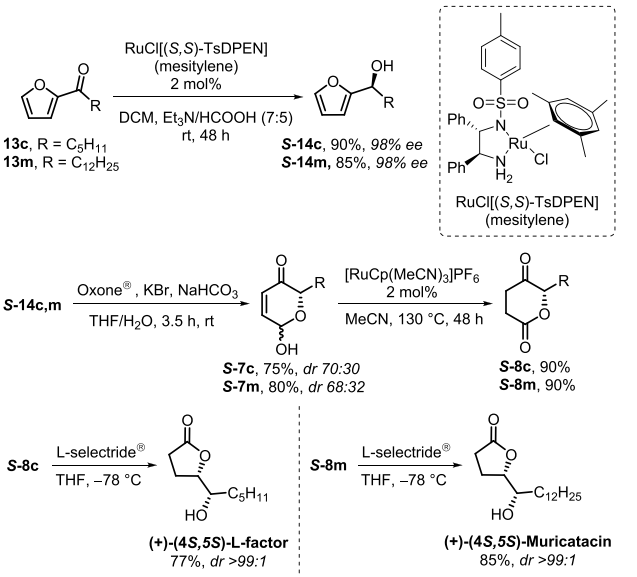

Achmatowicz rearrangement using Oxone as an oxidant rendered ***S*-7c** and ***S*-7m** in high yields (75 and 80%, respectively). The valerolactones ***S*-8c** and ***S*-8m** obtained after isomerization with $[RuCp(MeCN)_3]PF_6$ were subjected to reduction by L-selectride, which proceeded in a stereoselective manner and delivered L-factor and muricatacin as single (+)-(4*S*,5*S*) diastereoisomers without racemization in 77 and 85% yields, respectively.

We also subjected the Achmatowicz derivative ***S*-7m** to isomerization in the presence of 1 mol % of the bulkier $[RuCp^*(MeCN)_3]PF_6$ catalyst in MeCN under reflux. No formation of the desired lactone ***S*-8m** was observed, which is in accordance with our observation in that the isomerization reaction is highly influenced by the length of the alkyl substituents at C-6 in the Achmatowicz dihydropyranones.

A deuterium labeling study was undertaken to determine the mechanism of the Ru-catalyzed isomerization. To this end, we prepared **D-3** isotopically labeled at the hemiacetal position. To obtain information on the molecularity of the process, we performed a crossover experiment between **D-3** and **7b** and analyzed the products by mass spectrometry and NMR spectroscopy (Scheme 6A). The deuterium was transferred intramolecularly to form product **3D-4**, while deuterated

https://doi.org/10.1021/acscatal.2c04867
ACS Catal. 2023, 13, 1916−1925

Scheme 6. Deuterium Labeling Studies

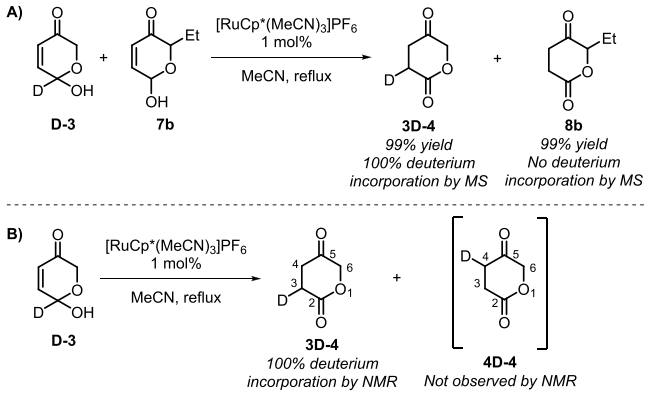

product **8b** was not observed. Noteworthy, by NMR experiments, we observed the incorporation of the deuterium solely at position 3, leading to the formation of product **3D-4** (Scheme 6B).

There are two generally accepted reaction pathways for the intramolecular transition metal-catalyzed redox isomerization of allylic alcohols that do not require an isolated metal-hydride precatalyst or its in situ generation. Both mechanisms operate via an intramolecular 1,3-hydride shift[57] with the involvement of either oxidative addition to the allylic C−H bond, forming a π-allyl metal-hydride complex[58−60] (Scheme 7A) or the

Scheme 7. Reported Mechanisms for the Transition Metal-Catalyzed Redox Isomerization of Allylic Alcohols

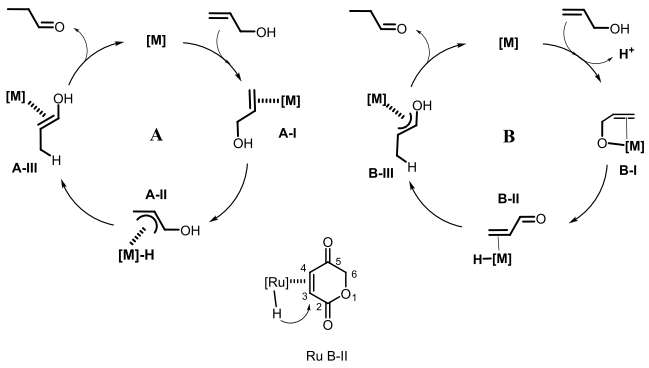

formation of metal alkoxide species[57,61−63] (Scheme 7B). The latter has been proposed in several instances for Ru(II) catalysis.[64,65] The hydride transfer (Scheme 7, A-II → A-III or B-II → B-III) in both previously established mechanisms should result in a regioselective deuterium incorporation at position 4, leading to compound **4D-4** (Scheme 6).

In our case, the exclusive formation of product **3D-4** suggests the formation of a type B-II Ru π-olefin complex that undergoes 1,4-hydride addition relative to the ketone governed by electrophilic and/or thermodynamic reasons (Scheme 7).

We then performed an Ir-catalyzed isomerization of **D-3** and observed a significant isotopic effect leading to a more sluggish reaction as compared to the non-deuterated substrate **3**. Despite product **3D-4** being predominantly formed, the formation of 25% **4D-4** was also evident (Scheme 8). Therefore, we suggest that the occurrence of competitive mechanisms that involve enolization of the lactone and consequent side reactions might be a possible cause for the lower yields of the Ir-catalyzed redox isomerization.

Scheme 8. [Ir(*cod*)MeO]$_2$/BiPy-Catalyzed Redox Isomerization of D-3

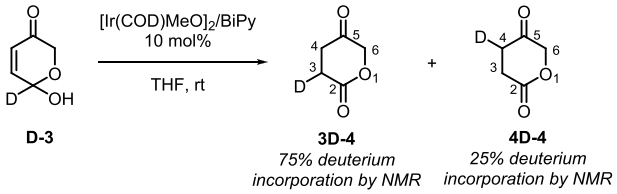

The preference for the transposition of the hydrogen from the hemiacetal to the β-position of the enone was studied by means of density functional theory[66] (DFT) calculations. The formation of a 16-electron complex is summarized in Figure 1, taking cation **A** as the starting point. The participation of such an intermediate is based on previous proposals[67,68] on the complexation of allyl alcohols to [RuCp*(MeCN)$_3$]PF$_6$. Such a process can be achieved by a dissociative ligand exchange and the participation of a ruthenium-complexed product that assists in the deprotonation of the starting allyl alcohol (vide infra - Figure 4). The displacement of an acetonitrile ligand from **A** is a favorable process as the 16-electron ruthenium complex **B** becomes 11.0 kcal/mol more stable than the initial cation. A β-hydride elimination with an energy barrier of 14.5 kcal/mol results in the formation of 16-electron ruthenium complex **D**, which is slightly less stable (2.2 kcal/mol) than the previous tridentate complex **B**. The β-agostic intermediate **C** represents a mid-way geometry between the transition states involved in the β-hydride elimination. The more exigent basis set (B3LYP-cc-pVTZ, SMD) revealed intermediate **C** as a step in the uphill β-hydride elimination process, although the same intermediate was flanked by two more energetic transition states **BC**‡ and **CD**‡ at the gas phase B3LYP-cc-pVDZ. The intermediate nature of species **C** in the β-hydride elimination process is demonstrated by the elongation of the C−H bond of the allylic hydrogen (1.184 vs 1.108 Å in **B**) and the formation of the Ru−H bond (1.957 Å). This is also accompanied by the weakening of the C−H bond as demonstrated by the lower Wiberg index (0.89 in **B** and 0.72 in **C**) due to a stronger interaction by the metal center with the migrating hydrogen atom (WI_{Ru-H} = 0 in **B** and WI_{Ru-H} = 0.13 in **C**). The hydride elimination is accompanied by a growing interaction of the metal center with the carbon atom during its change in the oxidation state. Such an event is visible in the structure of the four-membered intermediate **C** as the interaction between the metal and the carbon atoms is described by a 0.16 WI even though they are distant by d_{Ru-C} = 2.419 Å. The β-hydride elimination process with the migration of the hydride to the metal becomes complete with **D**. This intermediate has the hydride placed 2.538 Å away from the newly established sp^2 carbon (and a low 0.06 WI). The metal atom coordinates by η^2 with the newly created C═O bond as demonstrated by the distances from the metal to each atom of the carbonyl group (d_{Ru-O} = 2.106 and d_{Ru-C} = 2.230 Å) and considerable Wiberg index (WI_{Ru-O} = 0.55 and d_{Ru-C} = 0.44).

Other isomers of complex **D** that could form after decomplexation of the 5,6-dihydropyran-2,5-dione (DHPD) and further η^2 coordination were optimized to identify more stable isomers (Figure 2). Indeed, the coordination of DHPD to the ruthenium center by the carbon−carbon π system leads to considerably more stable complexes (**F**$_1$−**F**$_4$) than the η^2 coordination by the carbonyl π system (**D** and **E**) or by coordination to the oxygen lone pair (not shown). Although

https://doi.org/10.1021/acscatal.2c04867
ACS Catal. 2023, 13, 1916−1925

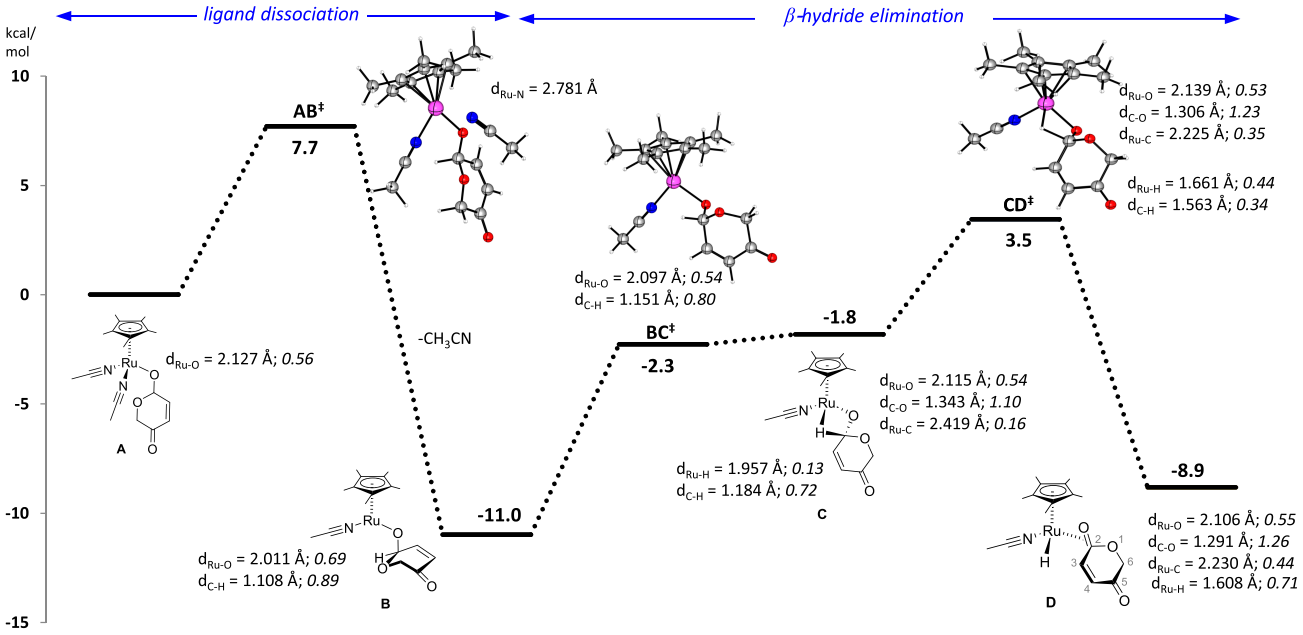

Figure 1. B3LYP/cc-pVTZ/SMD//B3LYP/cc-pVDZ relative free energies (kcal/mol) of stationary points along the *β*-hydride elimination pathway. Bond lengths (in Å) and Wiberg indexes (in italic) of relevant bonds are presented. The initial point (**A**) relates to the energy of the $[RuCp^*(MeCN)_2alcohol]^+$ cation.

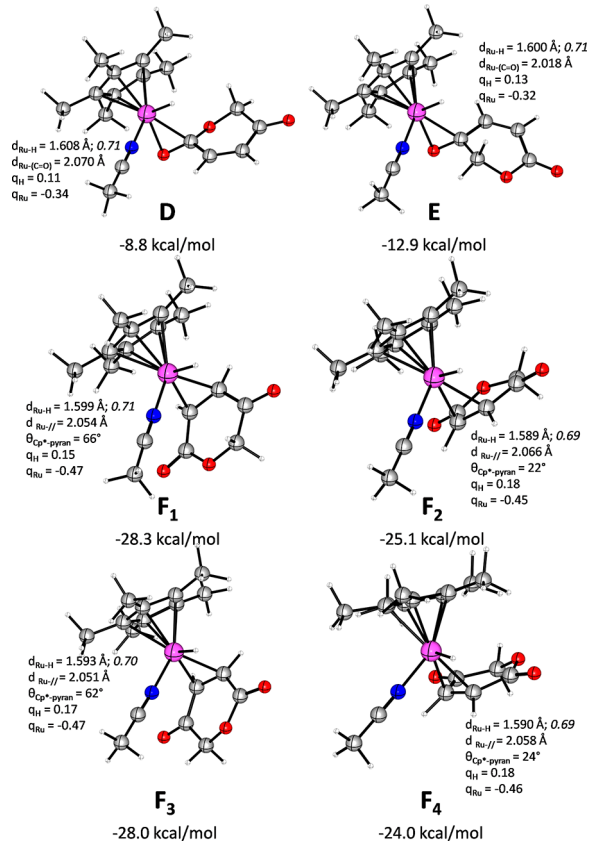

Figure 2. B3LYP/cc-pVTZ/SMD//B3LYP/cc-pVDZ relative free energies (kcal/mol) of stationary points for η^2 complexes of $RuCp^*H(CH_3CN)$ with DHPD. Bond lengths (in Å) and Wiberg indexes (in italic) of relevant bonds and selected atomic natural charges are presented.

the natural charge of the metal-bonded hydrogen atom is kept the same in the **D**, **E**, and **F** isomers shown (q_H = 0.11−0.18), the metal center becomes more negative when coordinated to the C═C bond (isomers **D** and **E**, q_{Ru} = −0.47 to −0.45) than when coordinated to the C═O bond (isomers **F**, q_{Ru} = −0.34 to −0.32). The stability of the complex upon coordination by the metal to the C═C bond was seen to be dependent on the orientation of DHPD to the pentamethylcyclopentadienyl unit. Geometries $\mathbf{F}_2$ and $\mathbf{F}_4$, both having co-planar DHPD and Cp* units, were determined to be 2.9−4.3 kcal/mol less stable than $\mathbf{F}_1$ and $\mathbf{F}_3$ in which the abovementioned rings are kept as far as possible.

Given the somewhat small differences in energies of the four isomers $\mathbf{F}_1$−$\mathbf{F}_4$, the reduction of DHPD by hydride delivery from the ruthenium complex was further studied (see the Supporting Information for further details). The two most energetically favorable paths are presented in Figure 3 in which conformer $\mathbf{F}_1$ is considered to undergo hydride delivery to the 4-position of DHPD and conformer $\mathbf{F}_4$ is to undergo hydride delivery to position 3. The energy barrier of the four-center transition state for the hydride delivery to the 3-position is 8.6 kcal/mol ($\mathbf{G}_4$) in contrast to the 13.7 kcal/mol required to reach intermediate $\mathbf{G}_1$. After complete delivery of the hydride to the *α*,*β*-unsaturated ketone, complex $\mathbf{H}_4$ is further stabilized in 1.6 kcal/mol upon bis-coordination of the ketone to the metal center in $\mathbf{I}_4$. The metal complex becomes even more stable as *O*-bound enolate $\mathbf{J}_4$ having a similar energy to $\mathbf{F}_4$. In contrast, the same type of coordination with the ester's carbonyl group in $\mathbf{I}_1$ does not warrant any stabilization to complex $\mathbf{H}_1$. Moreover, the isomerization from the *C*-bound enolate of the ester moiety $\mathbf{H}_1$ to its *O*-bound enolate $\mathbf{J}_1$ is 13.1 kcal/mol higher in energy than η^2 complex $\mathbf{F}_1$. An increase in the charge of the metal center during the hydride migration process indicates a change in the oxidation state of the metal as q_{Ru} changes from −0.46 in $\mathbf{F}_4$ to +0.04 in $\mathbf{J}_4$. The lack of stabilization in *O*-bound enolate $\mathbf{J}_1$ in comparison to its $\mathbf{J}_4$ congener is well in agreement with the observed isomerization of the isotopically labeled substrate.

https://doi.org/10.1021/acscatal.2c04867
ACS Catal. 2023, 13, 1916−1925

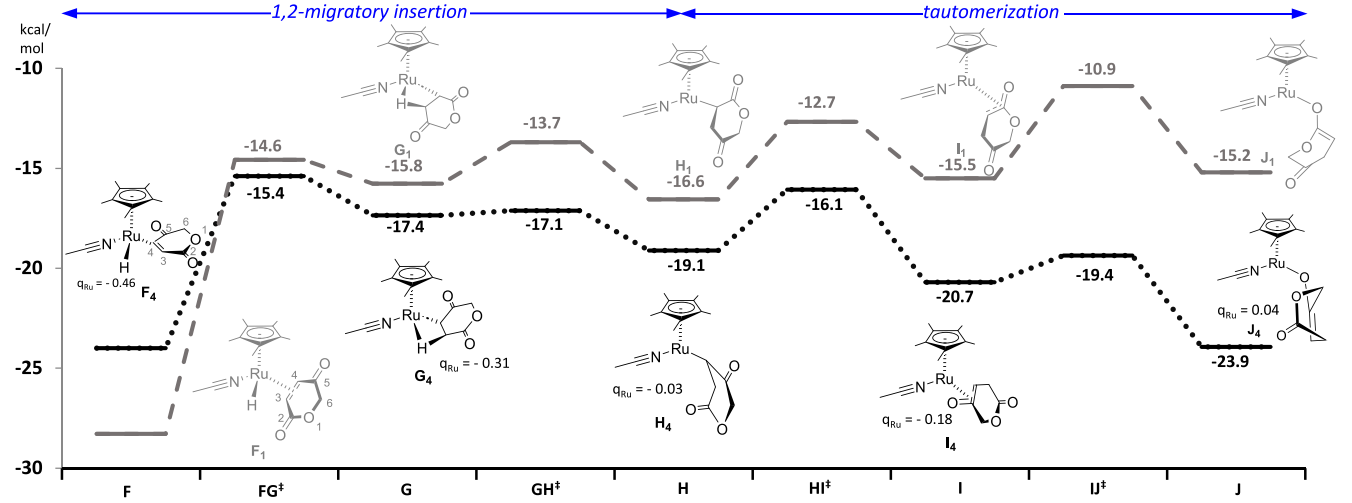

Figure 3. B3LYP/cc-pVTZ/SMD//B3LYP/cc-pVDZ relative free energies (kcal/mol) of stationary points along the pathways for the hydride delivery to the 3- and 4- positions of DHPD in black and gray, respectively. See the Supporting Information for further details and alternative pathways considered.

The release of the product occurs when another molecule of allyl alcohol is taken into the process (Figure 4). Such

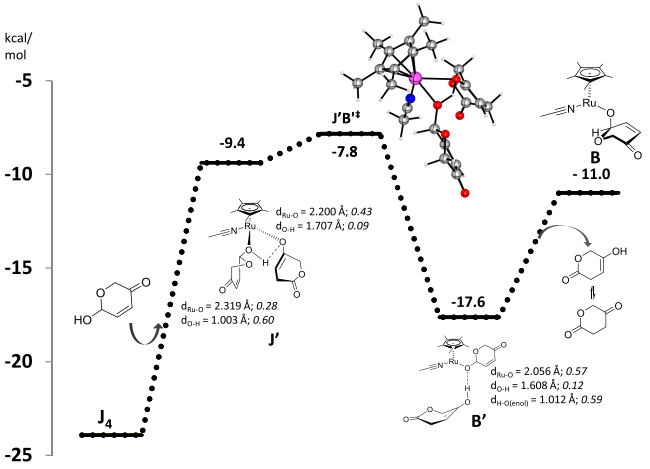

Figure 4. B3LYP/cc-pVTZ/SMD//B3LYP/cc-pVDZ relative free energies (kcal/mol) of proton exchange from allyl alcohol and regeneration of the catalytic active species. Bond lengths (in Å) and Wiberg indexes (in italic) of relevant bonds are presented.

molecule coordinates to ruthenium by the hydroxyl group to form intermediate **J′**, which ultimately increases the proton lability and proton transfer to the oxygen atom of the *O*-bound enolate via transition state **J′B′**‡. Despite the energy demand for the approaching allyl alcohol to the metal complex, the proton transfer barrier is only 1.6 kcal/mol, leading to a more stable complex **B′**, which readily releases the enol of the final product, and complex **B**, which is ready to undergo *β*-hydride elimination and close the catalytic cycle.

CONCLUSIONS

In summary, we have presented a new practical intramolecular Ru-catalyzed redox isomerization of Achmatowicz derivatives, which allows easy access to a range of important lactones. In doing so, we provided a new high-yielding route to the biorenewable monomer 4-ketovalerolactone (KVL), thus paving the way for its larger use in the design of new polymers. Furthermore, we utilized our findings in the synthesis of several biologically significant lactones and developed a new concise protective-group-free asymmetric synthesis of two natural products, namely, muricatacin and L-factor. The selectivity of the process, namely, that concerning the preference for the delivery of the hydride to a specific position of the unsaturated heterocycle, was verified by isotopic labeling and rationalized by computational means.

FUNDING

This work received financial support from the Bulgarian National Science Fund (BNSF) under the National Scientific Program "VIHREN" (grant no. КП-06-ДВ-1) and from the PT national funds (FCT/MCTES, Fundação para a Ciência e Tecnologia and Ministério da Ciência, Tecnologia e Ensino Superior) through the project nos. UIDB/50006/2020, UIDP/50006/2020, and PTDC/QUI-QOR/1131/2020. The project leading to this application received funding from the European Union's Horizon 2020 research and innovation program under grant agreement no. 951996.

ASSOCIATED CONTENT

Supporting Information

The Supporting Information is available free of charge at https://pubs.acs.org/doi/10.1021/acscatal.2c04867.

Experimental data (PDF)
Analytical and computational data (PDF)

AUTHOR INFORMATION

Corresponding Author

Svilen P. Simeonov − *Institute of Organic Chemistry with Centre of Phytochemistry, Bulgarian Academy of Sciences, Sofia 1113, Bulgaria; Research Institute for Medicines (iMed.ULisboa), Faculty of Pharmacy, Universidade de Lisboa, 1649-003 Lisbon, Portugal;* orcid.org/0000-0002-6824-5982; Email: svilen.simeonov@orgchm.bas.bg

Authors

Miroslav Dangalov − *Institute of Organic Chemistry with Centre of Phytochemistry, Bulgarian Academy of Sciences, Sofia 1113, Bulgaria*

https://doi.org/10.1021/acscatal.2c04867
ACS Catal. 2023, 13, 1916−1925

Adolfo Fernández-Figueiras − *Institute of Organic Chemistry with Centre of Phytochemistry, Bulgarian Academy of Sciences, Sofia 1113, Bulgaria*

Martin A. Ravutsov − *Institute of Organic Chemistry with Centre of Phytochemistry, Bulgarian Academy of Sciences, Sofia 1113, Bulgaria*

Ekaterina Vakarelska − *Institute of Organic Chemistry with Centre of Phytochemistry, Bulgarian Academy of Sciences, Sofia 1113, Bulgaria*

Maya K. Marinova − *Institute of Organic Chemistry with Centre of Phytochemistry, Bulgarian Academy of Sciences, Sofia 1113, Bulgaria*

Nuno R. Candeias − *LAQV-REQUIMTE, Department of Chemistry, University of Aveiro, 3810-193 Aveiro, Portugal; Faculty of Engineering and Natural Sciences, Tampere University, 33101 Tampere, Finland;* orcid.org/0000-0003-2414-9064

Complete contact information is available at: https://pubs.acs.org/10.1021/acscatal.2c04867

Author Contributions

⊥M.D. and A.F.-F. contributed equally. Conceptualization was done by S.P.S. Experimental methods were done by M.D., A.F.-F., M.A.R., E.V., M.K.M., and S.P.S. Computational methods were done by N.R.C. Funding acquisition was done by S.P.S. and N.R.C. The manuscript was written through contributions of all authors. All authors have given approval to the final version of the manuscript.

Notes

The authors declare no competing financial interest.

■ ACKNOWLEDGMENTS

The authors acknowledge the National Scientific Program "VIHREN" (grant no. КП-06-ДВ-1). N.R.C. thanks the FCT (Fundação para a Ciência e Tecnologia) for funding through the Scientific Employment Stimulus (no. CEECINST/00026/2018). This work received support from the PT national funds (FCT/MCTES, Fundação para a Ciência e Tecnologia and Ministério da Ciência, Tecnologia e Ensino Superior) through the project nos. UIDB/50006/2020, UIDP/50006/2020, and PTDC/QUI-QOR/1131/2020. The CSC-IT Center for Science Ltd., Finland, is acknowledged for the allocation of computational resources. The authors are grateful to the INFRAMAT project (part of the Bulgarian National Roadmap for research infrastructure, which is supported by the Bulgarian Ministry of Education and Science) for some of the research equipment that was used in this investigation. Dr. Joao Ravasco is acknowledged for the HRMS analysis.

■ REFERENCES

(1) Mariscal, R.; Maireles-Torres, P.; Ojeda, M.; Sádaba, I.; López Granados, M. Furfural: a renewable and versatile platform molecule for the synthesis of chemicals and fuels. *Energy Environ. Sci.* **2016**, *9*, 1144−1189.

(2) Li, X.; Jia, P.; Wang, T. Furfural: a promising platform compound for sustainable production of C4 and C5 Chemicals. *ACS Catal.* **2016**, *6*, 7621−7640.

(3) Lange, J.-P.; van der Heide, E.; van Buijtenen, J.; Price, R. Furfural − a promising platform for lignocellulosic biofuels. *ChemSusChem* **2012**, *5*, 150−166.

(4) Yan, K.; Wu, G.; Lafleur, T.; Jarvis, C. Production, properties and catalytic hydrogenation of furfural to fuel additives and value-added chemicals. *Renewable Sustainable Energy Rev.* **2014**, *38*, 663−676.

(5) Ma, Y.; Vemula, R.; Zhang, Q.; Wu, B.; O'Doherty, G. A. Achmatowicz approach to the asymmetric synthesis of (+)- and (−)-monanchorin. *Green Synth. Catal.* **2022**, *3*, 156−161.

(6) Li, N.; Zong, M.-H. (Chemo)biocatalytic upgrading of biobased furanic platforms to chemicals, fuels, and materials: a comprehensive review. *ACS Catal.* **2022**, *12*, 10080−10114.

(7) Bielski, R.; Grynkiewicz, G. Half a century with Achmatowicz rearrangement. *Tetrahedron* **2021**, *85*, No. 132058.

(8) Ghosh, A. K.; Brindisi, M. Achmatowicz reaction and its application in the syntheses of bioactive molecules. *RSC Adv.* **2016**, *6*, 111564−111598.

(9) Li, Z.; Tong, R. Catalytic Environmentally friendly protocol for achmatowicz rearrangement. *J. Org. Chem.* **2016**, *81*, 4847−4855.

(10) Deska, J.; Thiel, D.; Gianolio, E. The Achmatowicz rearrangement − oxidative ring expansion of furfuryl alcohols. *Synthesis* **2015**, *47*, 3435−3450.

(11) Achmatowicz, O.; Bukowski, P.; Szechner, B.; Zwierzchowska, Z.; Zamojski, A. Synthesis of methyl 2,3-dideoxy-DL-alk-2-enopyranosides from furan compounds: A general approach to the total synthesis of monosaccharides. *Tetrahedron* **1971**, *27*, 1973−1996.

(12) Simeonov, S. P.; Ravutsov, M. A.; Mihovilovic, M. D. Biorefinery via achmatowicz rearrangement: synthesis of pentane-1,2,5-triol from furfuryl alcohol. *ChemSusChem* **2019**, *12*, 2748−2754.

(13) Simeonov, S. P.; Lazarova, H. I.; Marinova, M. K.; Popova, M. D. Achmatowicz rearrangement enables hydrogenolysis-free gas-phase synthesis of pentane-1,2,5-triol from furfuryl alcohol. *Green Chem.* **2019**, *21*, 5657−5664.

(14) Liang, L.; Guo, L.-D.; Tong, R. Achmatowicz rearrangement-inspired development of green chemistry, organic methodology, and total synthesis of natural products. *Acc. Chem. Res.* **2022**, *55*, 2326−2340.

(15) Kim, S.; Oiler, J.; Xing, Y.; O'Doherty, G. A. De novo asymmetric Achmatowicz approach to oligosaccharide natural products. *Chem. Commun.* **2022**, *58*, 12913−12926.

(16) Dong, L.; Schill, H.; Grange, R. L.; Porzelle, A.; Johns, J. P.; Parsons, P. G.; Gordon, V. A.; Reddell, P. W.; Williams, C. M. Anticancer agents from the australian tropical rainforest: spiroacetals EBC-23, 24, 25, 72, 73, 75 and 76. *Chem. − Eur. J.* **2009**, *15*, 11307−11318.

(17) Zhu, L.; Talukdar, A.; Zhang, G.; Kedenburg, J. P.; Wang, P. G. A Divergent synthesis of uncommon sugars from furanaldehyde. *Synlett* **2005**, *2005*, 1547−1550.

(18) Harris, J. M.; Keränen, M. D.; Nguyen, H.; Young, V. G.; O'Doherty, G. A. Syntheses of four D- and L-hexoses via diastereoselective and enantioselective dihydroxylation reactions. *Carbohydr. Res.* **2000**, *328*, 17−36.

(19) Croatt, M. P.; Carreira, E. M. Probing the role of the mycosamine C2′-OH on the activity of amphotericin B. *Org. Lett.* **2011**, *13*, 1390−1393.

(20) Bartlett, S.; Hodgson, R.; Holland, J. M.; Jones, M.; Kilner, C.; Nelson, A.; Warriner, S. Exploiting predisposition in the stereoselective synthesis of mono-, bi- and tetracyclic oxygen heterocycles: Equilibration between, and trapping of, alternative di- and tetraacetals. *Org. Biomol. Chem.* **2003**, *1*, 2393−2402.

(21) Georgiadis, M. P.; Haroutounian, S. A.; Couladouros, E. A.; Apostolopoulos, C. D.; Chondros, K. P. Products from Furans. XVI . Novel synthetic routes to sympathomimetic amine analogues via 6-hydroxy-2H-pyran-3(6H)-ones. *J. Heterocycl. Chem.* **1991**, *28*, 697−703.

(22) Zhang, X.-X.; Zhang, Y.; Liao, L.; Gao, Y.; Su, H. E. M.; Yu, J.-S. Catalytic asymmetric isomerization of (homo)allylic alcohols: recent advances and challenges. *ChemCatChem* **2022**, No. e202200126.

(23) Scalambra, F.; Lorenzo-Luis, P.; de los Rios, I.; Romerosa, A. Isomerization of allylic alcohols in water catalyzed by transition metal complexes. *Coord. Chem. Rev.* **2019**, *393*, 118−148.

(24) Liu, T.-L.; Ng, T. W.; Zhao, Y. Rhodium-catalyzed enantioselective isomerization of secondary allylic alcohols. *J. Am. Chem. Soc.* **2017**, *139*, 3643−3646.
(25) Li, H.; Mazet, C. Iridium-catalyzed selective isomerization of primary allylic alcohols. *Acc. Chem. Res.* **2016**, *49*, 1232−1241.
(26) Liu, P. N.; Ju, K. D.; Lau, C. P. Highly efficient redox isomerization of allylic alcohols and transfer hydrogenation of ketones and aldehydes catalyzed by ruthenium complexes. *Adv. Synth. Catal.* **2011**, *353*, 275−280.
(27) Cadierno, V.; García-Garrido, S. E.; Gimeno, J.; Varela-Álvarez, A.; Sordo, J. A. Bis(allyl)−Ruthenium(IV) complexes as highly efficient catalysts for the redox isomerization of allylic alcohols into carbonyl compounds in organic and aqueous media: scope, limitations, and theoretical analysis of the mechanism. *J. Am. Chem. Soc.* **2006**, *128*, 1360−1370.
(28) Georgiadis, M. P.; Haroutounian, S. A.; Apostolopoulos, C. D. A convenient synthesis of 5-substituted 2-Pyrrolidinones via 2H-Pyran-3(6H)-ones. *Synthesis* **1991**, *1991*, 379−381.
(29) Wang, H.-Y.; Yang, K.; Bennett, S. R.; Guo, S.-r.; Tang, W. Iridium-catalyzed dynamic kinetic isomerization: expedient synthesis of carbohydrates from achmatowicz rearrangement products. *Angew. Chem., Int. Ed.* **2015**, *54*, 8756−8759.
(30) Liu, Y.-C.; Merten, C.; Deska, J. Enantioconvergent biocatalytic redox isomerization. *Angew. Chem., Int. Ed.* **2018**, *57*, 12151−12156.
(31) Liu, Y.-C.; Wu, Z.-L.; Deska, J. Coding synthetic chemistry strategies for furan valorization into bacterial designer cells. *ChemSusChem* **2022**, No. e202201790.
(32) Xu, S.; Wang, Y.; Hoye, T. R. Poly(4-ketovalerolactone) from levulinic acid: synthesis and hydrolytic degradation. *Macromolecules* **2020**, *53*, 4952−4959.
(33) Numata, A.; Hokimoto, K.; Takemura, T.; Katsuno, T.; Yamamoto, K. Plant constituents biologically active to insects. v. antifeedants for the larvae of the Yellow Butterfly, Eurema hecabe mandarina, in osmunda japonica. (1). *Chem. Pharm. Bull.* **1984**, *32*, 2815−2820.
(34) Cavé, A.; Chaboche, C.; Figadère, B.; Harmange, J. C.; Laurens, A.; Peyrat, J. F.; Pichon, M.; Szlosek, M.; Cotte-Lafitte, J.; Quéro, A. M. Study of the structure-activity relationships of the acetogenin of annonaceae, muricatacin and analogues. *Eur. J. Med. Chem.* **1997**, *32*, 617−623.
(35) Rieser, M. J.; Kozlowski, J. F.; Wood, K. V.; McLaughlin, J. L. Muricatacin: A simple biologically active acetogenin derivative from the seeds of annona muricata (annonaceae). *Tetrahedron Lett.* **1991**, *32*, 1137−1140.
(36) Wright, A. E.; Schäfer, M.; Midland, S.; Munnecke, D. E.; Sims, J. J. Lateral root inducing compounds from the bacterium Erwinia quercina: Isolation, structure and synthesis. *Tetrahedron Lett.* **1989**, *30*, 5699−5702.
(37) Gräfe, U.; Reinhardt, G.; Schade, W.; Krebs, D.; Eritt, I.; Fleck, W. F.; Heinrich, E. Isolation and structure of novel autoregulators from Streptomyces Griseus. *J. Antibiot.* **1982**, *35*, 609−614.
(38) Muller, C. J.; Kepner, R. E.; Webb, A. D. Lactones in wines - a review. *Am. J. Enol. Vitic.* **1973**, *24*, 5.
(39) Muller, C. J.; Maggiora, L.; Kepner, R. E.; Webb, A. D. Identification of two isomers of 4,5-dihydroxyhexanoic acid gamma lactone in Californian and Spanish flor sherries. *J. Agric. Food Chem.* **1969**, *17*, 1373−1376.
(40) Hur, J.; Jang, J.; Sim, J. A Review of the Pharmacological Activities and recent synthetic advances of γ-butyrolactones. *Int. J. Mol. Sci.* **2021**, *22*, 2769.
(41) Mao, B.; Fañanás-Mastral, M.; Feringa, B. L. Catalytic asymmetric synthesis of butenolides and butyrolactones. *Chem. Rev.* **2017**, *117*, 10502−10566.
(42) Avedissian, H.; Sinha, S. C.; Yazbak, A.; Sinha, A.; Neogi, P.; Sinha, S. C.; Keinan, E. Total synthesis of asimicin and bullatacin. *J. Org. Chem.* **2000**, *65*, 6035−6051.
(43) Pearson, W. H.; Hembre, E. J. A practical synthesis of (−)-Swainsonine. *J. Org. Chem.* **1996**, *61*, 7217−7221.
(44) Iwaki, S.; Marumo, S.; Saito, T.; Yamada, M.; Katagiri, K. Synthesis and activity of optically active disparlure. *J. Am. Chem. Soc.* **1974**, *96*, 7842−7844.
(45) Gräfe, U.; Eritt, I. On the biological inactivity of 4, 5-dihydroxy-n-decanoic acid-4-lactones. *J. Antibiot.* **1983**, *36*, 1592−1593.
(46) Wang, W.; Zhang, R.; Wang, J.; Tang, J.; Wang, M.; Kuang, Y. Antitumour activity of muricatacin isomers and its derivatives in human colorectal carcinoma Cell HCT116. *Anti-Cancer Agents Med. Chem.* **2020**, *20*, 254−263.
(47) Murcia, M.; Navarro, C.; Moreno, A.; Csaky, G. A. Naturally occurring δ-hydroxy-γ-lactones: muricatacins and related compounds. *Curr. Org. Chem.* **2010**, *14*, 15−47.
(48) Fernandes, R. A.; Bhowmik, A.; Choudhary, P. Muricatacin, a gateway molecule to higher acetogenin synthesis. *Chem. − Asian J.* **2020**, *15*, 3660−3681.
(49) Fernandes, R. A.; Gangani, A. J.; Kumari, A.; Kumar, P. A Decade of muricatacin synthesis and beyond. *Eur. J. Org. Chem.* **2020**, *2020*, 6845−6858.
(50) Chaudhari, D. A.; Ingle, A. B.; Fernandes, R. A. A concise synthesis of (4R,5R)-(−)-muricatacin and (4R,5R)-l-(−)-factor from d-glucono-δ-lactone. *Tetrahedron: Asymmetry* **2016**, *27*, 114−117.
(51) Srećo, B.; Benedeković, G.; Popsavin, M.; Hadžić, P.; Kojić, V.; Bogdanović, G.; Divjaković, V.; Popsavin, V. Heteroannelated (+)-muricatacin mimics: synthesis, antiproliferative properties and structure−activity relationships. *Tetrahedron* **2011**, *67*, 9358−9367.
(52) Ghosal, P.; Kumar, V.; Shaw, A. K. A chiron approach to the total synthesis of cytotoxic (+)-muricatacin and (+)-5-epi-muricatacin from d-ribose. *Carbohydr. Res.* **2010**, *345*, 41−44.
(53) Dong, H.-B.; Yang, M.-Y.; Liu, B.; Wang, M.-A. Concise stereoselective total synthesis of (+)-muricatacin and (+)-epi-muricatacin. *J. Asian Nat. Prod. Res.* **2014**, *16*, 847−853.
(54) Sabitha, G.; Chandrashekhar, G.; Vasudeva Reddy, D.; Yadav, S. J. Synthesis of (+)-(4S,5S)-Muricatacin via Pd-catalyzed stereospecific hydroxy substitution reaction of γ,δ-epoxy α,β-unsaturated ester with $B(OH)_3$. *Lett. Org. Chem.* **2012**, *9*, 344−346.
(55) Ohkuma, T.; Koizumi, M.; Yoshida, M.; Noyori, R. General asymmetric hydrogenation of hetero-aromatic ketones. *Org. Lett.* **2000**, *2*, 1749−1751.
(56) Fujii, A.; Hashiguchi, S.; Uematsu, N.; Ikariya, T.; Noyori, R. Ruthenium(II)-catalyzed asymmetric transfer hydrogenation of ketones using a formic acid−triethylamine mixture. *J. Am. Chem. Soc.* **1996**, *118*, 2521−2522.
(57) Uma, R.; Crévisy, C.; Grée, R. Transposition of allylic alcohols into carbonyl compounds mediated by transition metal complexes. *Chem. Rev.* **2003**, *103*, 27−52.
(58) van der Drift, R. C.; Bouwman, E.; Drent, E. Homogeneously catalysed isomerisation of allylic alcohols to carbonyl compounds. *J. Organomet. Chem.* **2002**, *650*, 1−24.
(59) Hiroya, K.; Kurihara, Y.; Ogasawara, K. Asymmetrization of meso 1,4-enediol ethers by isomerization with a chiral binap−RhI catalyst. *Angew. Chem., Int. Ed.* **1995**, *34*, 2287−2289.
(60) Bergens, S. H.; Bosnich, B. Homogeneous catalysis. Catalytic production of simple enols. *J. Am. Chem. Soc.* **1991**, *113*, 958−967.
(61) Kress, S.; Johnson, T.; Weisshar, F.; Lautens, M. Synthetic and mechanistic studies on the rhodium-catalyzed redox isomerization of cyclohexa-2,5-dienols. *ACS Catal.* **2016**, *6*, 747−750.
(62) Batuecas, M.; Esteruelas, M. A.; García-Yebra, C.; Oñate, E. Redox isomerization of allylic alcohols catalyzed by osmium and ruthenium complexes containing a cyclopentadienyl ligand with a pendant amine or phosphoramidite group: X-ray structure of an η3-1-hydroxyallyl-metal-hydride intermediate. *Organometallics* **2010**, *29*, 2166−2175.
(63) Ahlsten, N.; Martín-Matute, B. Rhodium-catalysed coupling of allylic, homoallylic, and bishomoallylic alcohols with aldehydes and n-tosylimines: insights into the mechanism. *Adv. Synth. Catal.* **2009**, *351*, 2657−2666.
(64) Cadierno, V.; Crochet, P.; Gimeno, J. Ruthenium-catalyzed isomerizations of allylic and propargylic alcohols in aqueous and

https://doi.org/10.1021/acscatal.2c04867
ACS Catal. 2023, 13, 1916−1925

organic media: applications in synthesis. *Synlett* **2008**, *2008*, 1105−1124.
(65) van der Drift, R. C.; Vailati, M.; Bouwman, E.; Drent, E. Two reactions of allylic alcohols catalysed by ruthenium cyclopentadienyl complexes with didentate phosphine ligands: isomerisation and ether formation. *J. Mol. Catal. A: Chem.* **2000**, *159*, 163−177.
(66) Parr, R. G.; Weitao, Y. *Density-Functional Theory of Atoms and Molecules*. Oxford University Press: 1995, 1−333, DOI: 10.1093/oso/9780195092769.001.0001.
(67) Trost, B. M.; Kulawiec, R. J. Chemoselectivity in the ruthenium-catalyzed redox isomerization of allyl alcohols. *J. Am. Chem. Soc.* **1993**, *115*, 2027−2036.
(68) Slugovc, C.; Rüba, E.; Schmid, R.; Kirchner, K. Improved efficiency of the ruthenium-catalyzed redox isomerization of allyl alcohols. *Organometallics* **1999**, *18*, 4230−4233.

https://doi.org/10.1021/acscatal.2c04867
ACS Catal. 2023, 13, 1916−1925